

FINITE ELEMENT MODELLING OF SUBMERGED ARC WELDING PROCESS FOR A SYMMETRIC T-BEAM

MODELIRANJE POSTOPKA OBLOČNEGA VARJENJA POD PRAŠKOM SIMETRIČNEGA T-NOSILCA Z METODO KONČNIH ELEMENTOV

Osman Culha

Celal Bayar University, Engineering Faculty, Department of Materials Engineering, Muradiye Campus, Manisa, Turkey
osman.culha@cbu.edu.tr

Prejem rokopisa – received: 2013-04-11; sprejem za objavo – accepted for publication: 2013-06-10

Metallurgical welding joints are extensively used in the fabrication industry, including ships, offshore structures, steel bridges and pressure vessels. The merits of such welded structures include a high joint efficiency, water and air tightness, and low fabrication costs. However, residual stresses and distortions can occur near the weld bead due to localized heating by the welding process and subsequent rapid cooling. This paper is focused on deriving a simulation solution to predict the design parameters, such as the temperature-stress distribution, the approximate gradient and the nodal displacement on the plates during the process of submerged arc welding (SAW). During the construction of an AH 36 quality T-beam profile using the SAW process, thermal residual stress and distortion occurs due to heat fusion from the source to the joint part of the symmetric T-beam. The value of the design parameter is achieved by performing a thermal elasto-plastic analysis using finite-element techniques. Furthermore, this investigation provides an available process analysis to enhance the fabrication process of welded structures.

Keywords: submerged arc welding (SAW), finite element modelling (FEM), stress-temperature distribution

Metalurško varjeni spoji se splošno uporabljajo v industriji, vključno z ladjedelništvom, za naftne ploščadi, jeklene mostove in tlačne posode. Prednosti takih varjenih konstrukcij so velika zmogljivost spoja, tesnost za vodo in zrak, nizki proizvodni stroški. Vendar pa se v okolici kopeli zvara zaradi lokalnega segrevanja in hitrega ohlajanja lahko pojavijo zaostale napetosti in izkrivljanje. Članek je osredinjen na izpeljavo rešitve simulacije za predvidenje parametrov kot so: razporeditev temperature – napetosti, približek gradienta in izkrivljanja vozlov na ploščah med postopkom obločnega varjenja pod praškom (SAW). Med sestavljanjem AH 36 kvalitete T-nosilca s postopkom SAW se pojavijo termične zaostale napetosti in izkrivljanja zaradi toplote zlivanja od vira do spojnega mesta simetričnega T-nosilca. Vrednosti parametrov so dobljene z izvajanjem termične elasto-plastične analize s tehniko končnih elementov. Poleg tega ta preiskava omogoča analizo procesa za pospešitev izdelave varjenih konstrukcij.

Ključne besede: obločno varjenje pod praškom (SAW), modeliranje z metodo končnih elementov (FEM), razporeditev napetosti – temperature

1 INTRODUCTION

Metallurgical welding joints are extensively used in the fabrication industry, which includes ships, offshore structures, steel bridges and pressure vessels. Among the merits of such welded structures are a high joint efficiency, water and air tightness, and low fabrication costs. However, residual stresses and distortions can occur near the weld bead due to localized heating by the welding process and subsequent rapid cooling. Additionally, phase transformations that occur in the weld metal and adjacent heat-affected zone (HAZ), e.g., in structural steels, contribute to the evolution of residual stress. Stress regions near the weld may promote brittle fractures, fatigue, or stress-corrosion cracking. Meanwhile, residual stresses in the base plate may reduce the buckling strength of the structure members.¹ The inherent characteristics of weldments, such as metallurgical or geometrical defects, the presence of stress raisers and heterogeneous material properties, make them particularly vulnerable to failure. In material selection it is general practice to specify weld metals with strengths

higher than those of the parent plate. This overmatching policy is thought to be able to offset potential problems, such as a reduced toughness and the presence of defects in the weld metals.² Therefore, the residual stresses of welding must be minimized to control them according to the respective requirements. Previous investigators developed several methods, including heat treatment, hammering, preheating, vibration stress relieving, and weld sequencing, to reduce the residual stresses attributed to welding.³⁻⁵ As known, many welded structures that cannot be subjected to post-weld manufacturing measures after the welding contain residual stresses of varying degree that can result in unintended deformations of the welded component, increase the susceptibility to hydrogen-induced cold cracking, and also combine with tensile stresses experienced during service to promote brittle fracture, fatigue failure, and stress-corrosion cracking. Thus, developing an available welding sequence and accurately predicting the welding residual stresses for a welds system are necessary in order to achieve the safest design.¹⁻⁹

On the other hand, traditional methods for welding-induced residual stress and strain characterization are mainly experimental, and include hole drilling, X-ray, neutron diffraction, ultrasonic and demountable mechanical gauge measurement. However, the application of these methods in practice is usually limited by either their cost or accuracy. Numerical simulations based on finite-element modelling are used to study the influence of welding sequences on the distribution of the residual stress and distortion generated when welding a flat-bar stiffener to a steel plate. The simulation consists of sequentially coupled thermal and structural analyses using an element birth-and-death technique to model the addition of weld metal to the workpiece. The temperature field during welding and the welding-induced residual stress and distortion fields are predicted and the results are compared with experimental measurements and analytical predictions.^{10,11}

The intense heat input from the welding process and the molten steel, which is deposited into the joint, contribute to the thermal expansion and contraction of the heated parts. Also, residual stresses released in the rolled and raw-cut material will have some influence on the final shape of the beam. If the welding is carried out on only one side of the web the plate will bend upwards and sideways (sweep and camber). If two welds are made simultaneously, one on each side of the web, the beam tends only to exhibit beam camber due to the shrinkage produced after welding. Distortion can be minimized in symmetrical designs by applying the heat into the material in a symmetrical manner. The remaining distortion on the final part can rarely be tolerated in subsequent assemblies and must be eliminated with either thermal or mechanical methods. Both mechanical and thermal

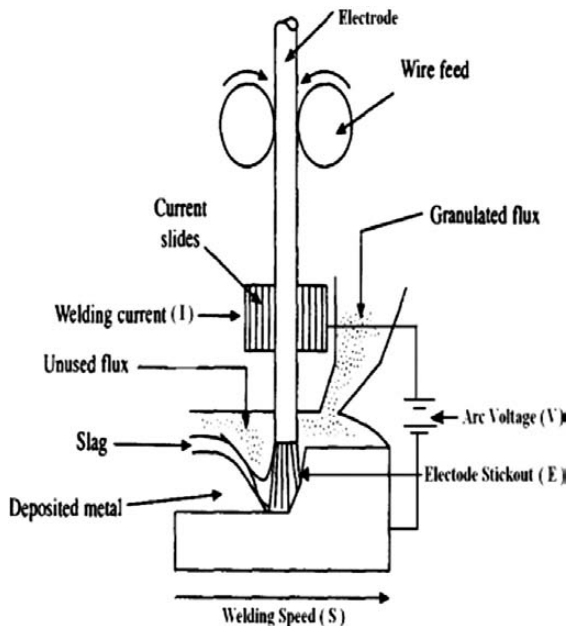


Figure 1: Schematics of submerged arc welding process
Slika 1: Shematski prikaz obločnega varjenja pod praškom

straightening techniques are used to straighten the beams subjected to plate shrinkage. Mechanical straightening requires large, expensive machines, which produce process "wrinkles". As with thermal straightening, this technique adds another step to the production line for beams. Thermal straightening requires that the opposite (upper) side of the beam is heated – which later induces a compensating shrinkage. This is supposed to compensate for the initial shrinkage induced during the welding process mentioned above and can be carried out with a propane burner or induction line heating. In accordance with these explanations, the aims of the study were to obtain the temperature, stress and displacement region of a submerged arc welding (SAW) process for welded T-beam dimensions of 180 mm × 28 mm and 630 mm × 14 mm, AH 36 quality steel bars using the finite-element method.

2 SUBMERGED ARC WELDING (SAW) PROCEDURES FOR FLAT BARS

Submerged arc welding is a method in which the heat required to fuse the metal is generated by an electric current passing between the welding wire and the workpiece. The tip of the welding wire, the arc and the weld area are covered by a layer of granular flux. A hopper and a feeding mechanism are used to provide a flow of flux over the joint being welded. A conveyor tube is

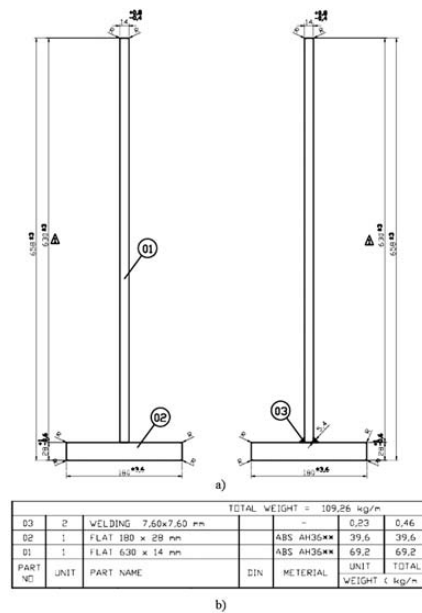


Figure 2: Dimensional representation of steel bars for finite-element model analysis

Slika 2: Predstavitev dimenzij jeklenih palic, uporabljenih za analizo z metodo končnih elementov

Table 1: Process parameters of submerged arc welding (SAW)

Tabela 1: Procesni parametri pri obločnem varjenju pod praškom (SAW)

Wire diameter (mm)	Amperage (A)	Voltage (V)	Welding speed (mm/min)
2.4	780	28	740

provided to control the flow of the flux and is always kept ahead of the weld zone to ensure an adequate supply of flux ahead of the arc. The intense heat evolved by the passage of the electric current through the welding zone melts the end of the wire and the adjacent edges of the workpieces, creating a puddle of molten metal. The puddle is in a liquid state and is turbulent. For this reason any slag or gas bubble is quickly swept to the surface. The flux completely shields the welding zone from any contact with the atmosphere. Additionally, SAW can use a much higher heat input and has slower solidification and cooling characteristics. Also, the silicon content will be much higher in submerged arc welding if care is not exercised in selecting the proper flux material. SAW can be used for the welding of materials in higher gauges and has the advantage of a high weld-metal quality and a smooth and uniform weld finish. The deposit rate, deposition efficiency and the weld speed are high. This means that smoke and arc flash are absent in this procedure (**Figure 1**).

According to these advantages of the SAW process, it was applied to two different steel plates (as shown in **Figure 2**; 180 mm × 28 mm and 630 mm × 14 mm) at Özkan Iron Steel Industry Co., Ltd. for the production of a symmetrical T-beam process. The SAW production-line parameters such as wire diameter, amperage, voltage and welding speed are listed **Table 1**. In particular, since the heat input amount per millimetre was affected by these parameters, they were controlled and modified depending on the dimensions of the steel plate.

3 FINITE-ELEMENT MODELLING OF WELDING FLAT BARS

The simulation technologies were developed in accordance with the development of computers. In many applications, the numerical simulation is applied to save costs. In the field of the welding, the numerical simulations were proposed and applied to the practical field in order to determine the welding conditions. The accuracy of the dimensions after the welding of the steel structure becomes an important factor for the product costs. The dimensions become inaccurate due to the welding distortion. Therefore, the control of the welding distortion is demanded in the steel structure welding so as to improve the productivity. For this purpose, an estimation of the amount of deformation is needed and its behaviour is investigated in this study.

The finite-element modelling (FEM) procedure for SAW was used to determine: a) the thermal stress formation and distribution, b) the temperature gradient, c) the deformation characteristics and d) the thermal straightening regions of the produced T-beam by welding. The SAW process under consideration was applied for the manufacture of a T-beam 180 mm × 28 mm and 630 mm × 14 mm steel plates, as shown in **Figure 3**. A two-dimensional (2D) FE model was used to investigate the detailed residual stress and strain distributions around

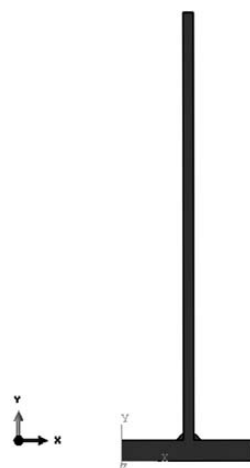


Figure 3: 2D model assembly of FE analysis
Slika 3: 2D modelni sestav za FE-analizo

the welded region of the T-beam. Therefore, the FE model 2D coupled temperature-displacement transient model was structured for the dimensions of the real steel plates. Additionally, the same thermal properties of the base and weld metals, such as the thermal conductivity, convection, expansion and the specific heat capacity, were taken for this analysis.

On the other hand, the yield strengths of the base and weld metals were taken at room temperature. The

Table 2: Composition of the steel used in the experiments
Tabela 2: Sestava jekla, uporabljenega pri poskusu

Material	C	Si	Mn	Cu	Al	V	P	S
AH 36	0.14	0.20	0.90	0.25	0.027	0.07	0.028	0.030

Table 3: Thermal and mechanical properties of AH 36 quality steel¹²
Tabela 3: Toplotne in mehanske lastnosti jekla AH 36¹²

Temperature, °C	Elastic Modulus, GPa	Poisson ratio, ν	Thermal Conductivity, K/W/(m °C)	Specific heat, J/(kg °C)	Thermal expansion coefficient, $\alpha/(10^{-6}/^{\circ}\text{C})$	Thermal convection coefficient, h/W/(m ² °C)
20	207	0.30	52	485	11.8	3.2
100	202	0.31	50	486	11.8	5.5
200	200	0.33	48	495	12.1	6.3
300	198	0.34	45	513	12.7	6.8
400	181	0.36	42	532	13.2	7.4
500	112	0.38	38	555	13.7	7.7
600	65	0.40	34	586	14.2	7.8
700	42	0.42	30	636	14.7	8.1
800	33	0.44	27	683	14.8	8.3
900	24	0.46	26	698	14.7	8.5
1000	13	0.48	28	698	14.7	8.6
1100	7	0.48	30	698	14.7	8.7
1200	7	0.48	31	698	14.7	8.8
1300	7	0.47	32	698	14.7	8.9
1400	7	0.47	34	698	14.7	9.0
1450	7	0.47	35	698	14.7	9.1
1500	7	0.47	95	698	14.7	9.2

Young's modulus and Poisson's ratio variations were assumed to be the same in the base and weld metals between 40 °C and 1450 °C.^{10,12} The Von Mises yield criterion and the associated flow rule were used together with kinematic hardening and a bilinear representation of the stress – strain curve. Kinematic hardening is believed to be the best model that can simulate the reverse plasticity and Bauschinger effect that is expected to occur during multipass welding. The density of both materials was assumed to be constant at a value of 7800 kg/m³. The composition of the AH 36 quality steel plates and weld metal used in the T-beam production is shown in **Table 2** and the properties used for the modelling of the temperature distributions and distortions are listed in **Table 3**.

Furthermore, creating the mesh design of the entire model was very important, especially when the problem had different thermal regions. So, the elements were finest in the welded area and became coarser away from the steel plates. In **Figure 4**, the welded regions of the steel plates were partitioned and meshed as the structured elements type and numbered as CPE4T: A4-node plane strain thermally coupled quadrilateral, bilinear displacement and temperature with 2000. In the region away from the location of the weld, the temperature gradient is significantly lower and the mesh was then made less dense in this region to reduce the number of degrees of freedom and thus the time required for the solution.

4 RESULTS AND DISCUSSION

4.1 Thermal history

A temperature-displacement analysis of the symmetrical T-beam welding with the given welding condition was performed using the 2D finite-element method. During this step, the temperature histories for each node were computed during the multipass welding process. Ogawa et al.¹³ states that the weld pass can be divided into a number of small parts (mesh blocks) with the same

length to simulate the deposition of the weld metal. In each weld pass, the volume of the moving heat source is equal to that of these elements composing the corresponding weld bead in one mesh block. The elements involved in each block are successively activated and then heated to model the moving heat source. However, since the main aim of study was to obtain the temperature gradient, distributions and thermal stress formation for whole body of the welded T-beam, a cooling procedure was applied to the welding zone from 1450 °C to 40 °C as soon as the welding process for the steel plates was finished. In this way the temperature gradient-distribution and the thermal stress-deformation amount, owing to cooling to room temperature, and the thermal expansion can be achieved using the finite-element model with the transient temperature-displacement analysis. According to this cooling procedure, the temperature contours of the weldments are shown in **Figures 5a** and **5b**. It indicated that the grey region was the welding place and its temperature was 1450 °C. When the cooling step of the symmetrical T-beam started and the temperature reduced from 1450 °C to 40 °C in 377 increments, the temperature distributions and thermal gradient took place from the cross-section of the welding region to flat bars, as shown in **Figures 6a** and **6b**. According to the nodal temperature variation versus time results, as graphically represented in **Figure 6a**, for example, at the node 348 (near the bottom plate), the reduction of the temperature from 1450 °C to 40 °C is faster than for the other nodes because of the cold bottom plate. So as the location of the temperature measurement changed from near the bottom plate to the centre of the welding region, the reduction of the temperature rate decreased and the cooling effect on the thermal gradient was small. On the other hand, the temperature distribution of the bottom steel plate is shown in **Figure 6b**. In accordance with the results, the temperature is increased from 40 °C to 88 °C at the node 145 (near the welding region) due to the heat diffusion from the welding region to the bottom steel plate over time. In addition, the temperature increase of

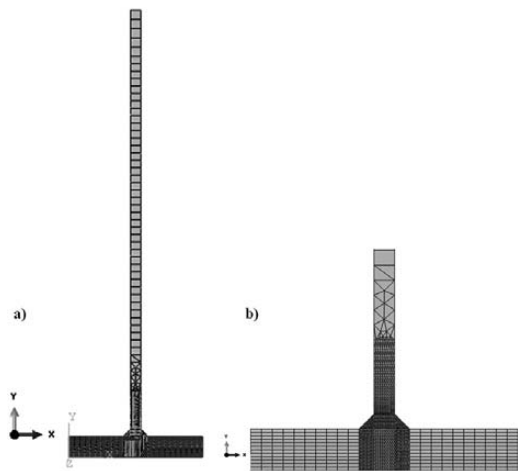


Figure 4: Mesh designs of 2D symmetrical welded T-beam: a) normal view and b) magnified view of welded region

Slika 4: Postavitev mreže 2D simetrično varjenega T-nosilca: a) normalen pogled, b) povečano področje zvara

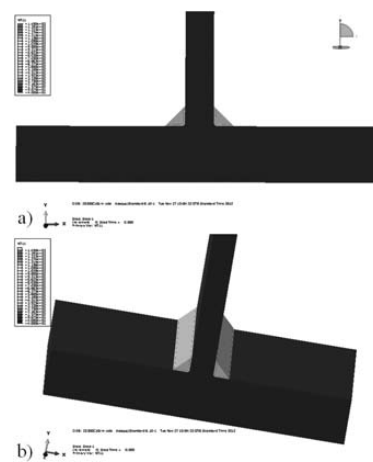


Figure 5: Temperature contour of welded region for: a) 2D model and b) representation of extruded 2D model

Slika 5: Kontura temperaturnega področja varjenja za: a) 2D model in b) ekstrudiran 2D model

the surface of the bottom steel plate is slowed down as it moves away from the source region (from node 145 to node 137).

4.2 Mechanical analysis

The same finite-element mesh as used in the thermal analysis was employed in the mechanical analysis. The analysis was conducted using temperature histories computed with the thermal analysis as the input information. Similar to the thermal analysis, in the mechanical analysis, the temperature-dependent mechanical properties,^{10,12,13} such as Young’s modulus, yield strength and thermal expansion coefficient, are employed. The elastic

strain-stress relationship is modelled using the isotropic Hooke’s law, and the plastic behaviour is considered through the Von Mises criterion. According to the counter analysis of the welding region as represented in **Figure 7a**, the nodal stress distribution shows that the thermal residual stress exceeded the yield stress of the welding material and the region is plastically deformed (stress exceeded 350 MPa). In detail, it can be seen that the nodal stress distribution is decreased from node 145 to node 142, as approximately 280 MPa to 70 MPa with time. When the temperature gradient effect started to disappear at the surface of the bottom steel plate (move away from the welding region), the thermal stress formation began to reduce, as shown in **Figure 7b**.

In this study an elastic-perfectly-plastic material model is used with Von Mises failure criteria and the

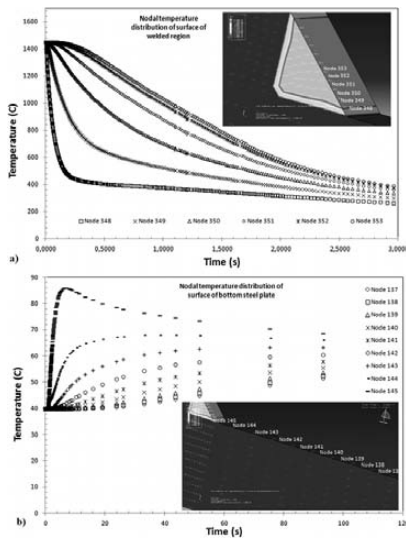


Figure 6: Nodal temperature distributions of: a) welding zone and b) surface of bottom steel plate for coupled temperature-displacement analysis

Slika 6: Rasporeditev temperaturnih vozlov: a) področje zvara in b) površina spodnje plošče za skupno analizo temperatura – izkrivljanje

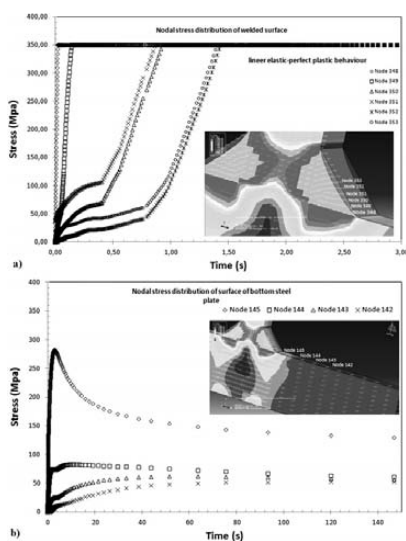


Figure 7: Von Mises stress formation and distribution stress distribution of: a) welding surface and b) bottom steel plate

Slika 7: Nastanek in rasporeditev Misesovih napetosti: a) varjena površina, b) spodnja jeklena plošča

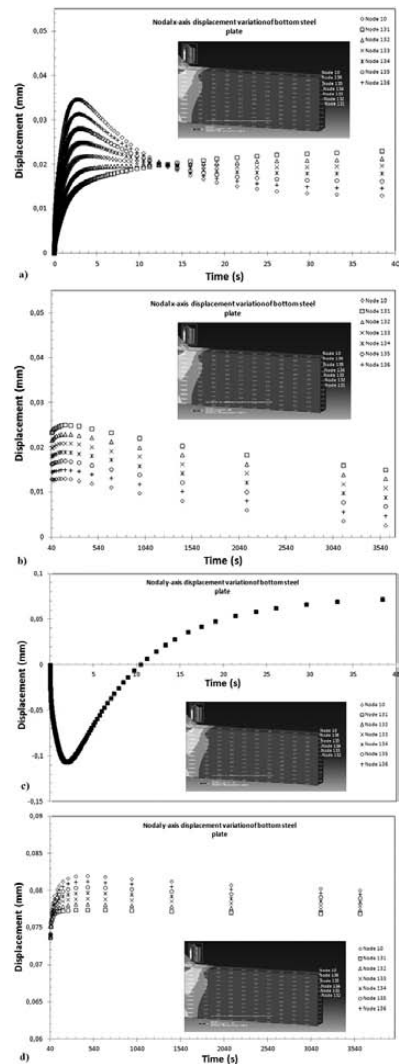


Figure 8: Nodal x-axis displacement variation of bottom steel plate between: a) 0–40 s, b) 40–3600 s after welding, c) nodal y-axis displacement variation of bottom steel plate between 0–40 s, d) 40–3600 s after welding

Slika 8: Variiranje izkrivljanj vozlov po x-osi na spodnji plošči: a) med 0–40 s, b) 40–3600 s po varjenju, c) variiranje izkrivljanj vozlov po y-osi na spodnji plošči med 0–40 s, d) 40–3600 s po varjenju

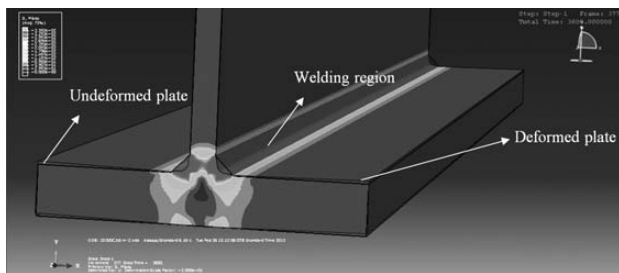


Figure 9: Deformed and undeformed model representation of welding using superimposed plot option of finite-element simulation

Slika 9: Predstavitev modela, deformiranega in nedeformiranega, pri varjenju s predpostavko možnosti simulacije z metodo končnih elementov

associated flow rule, which states that the plastic flow is orthogonal to the yield surface. Nonlinearities due to the large strain and displacement are considered. Strain hardening is not included and was also neglected in several previous studies.^{14,15} Experiments by Karlsson and Josefson¹⁶ showed a nearly ideal plastic behaviour for the material at temperatures above 800 °C. Since most plastic strains during welding occur at high temperature, this indicates that a perfectly plastic behaviour is suitable.¹⁰ So, the bottom plate of the welded material model has a displacement due to the thermal gradient, the stress and the strain distribution with time. According to the results of the finite-element simulation of the model, the x -axis nodal displacement (node number system: 10, 131, 132, 133, 134, 135 and 136) of the bottom steel plate is illustrate in **Figure 8a**: 40 s after welding and **Figure 8b**: 40–3600 s after welding. **Figures 8a** and **8b** explain that when the cooling procedure began at the welding region, the nodal displacement of the bottom-edge steel plate was firstly increased (positive direction) from starting point to 0.034 mm until 13 s, then decreased to 0.015 mm at the end of the cooling step. On the other hand, the y -axis net nodal displacement of the bottom region after 2 s, between 2–10 s and 10–3600 s was decreased to the -0.11 mm (negative direction), increased to the 0.0 point and increased form 0.0 point to the $+0.081$ mm, respectively. So a detailed analysis showed that the thermal expansion and the stress caused a deformation at the welding region and joint steel plate as shown in **Figure 8**. The deformed and undeformed bottom steel plate are represented in contours in **Figure 9**. It is clear that the bottom steel plate had a deformation depending on the thermal expansion of the welding region and the heat fusion from the source to the steel joints using a superimposed plot option of the analysis.

5 CONCLUSION

A finite-element analysis of the Submerged Arc Welding (SAW) process was applied to the T-beam joint of AH 36 quality steel plates to obtain the temperature history, thermal gradient, stress distribution and nodal displacement of the 2D model. According to the analysis, the following time-dependent results were obtained:

The temperature gradient and the thermal history of model were decreased from the welding region to the bottom steel plate, as represented graphically and with contours. The temperature decreased from 1450 °C to 40 °C at the welding zone and increased from 40 °C to 86 °C at the surface of the bottom steel plate.

In this research a 2D model was constructed as 2D and extruded to 3D. According to the analysis results the formation of the thermal stress at the welding zone exceeded the yield strength of material, and at 350 MPa plastic deformation occurred. When the cooling procedure of the welding finished, the graphical and contour representation showed that the bottom steel plate of the joints had a shrinkage effect due to the thermal stress. In addition, the thermal stress decreased from 350 MPa to approximately 80 MPa away from the welding zone.

The nodal displacement of the model revealed that the x and y axes net displacements of the bottom steel plate were 0.015 mm and 0.081 mm, respectively.

Acknowledgement

The author wishes to thank The Scientific and Technological Research Council of Turkey (TUBITAK-1501) for the financial support of the project titled and numbered as: Design and developed of thermal straightening machine using induction heating for welding application of steel joints and 3110745, respectively. The author would also like to thank the project team of Ozkan Iron and Steel Industry Co. Ltd.; Hakan Erçay and Serhat Turgut for their technical facilities.

6 REFERENCES

- T. L. Teng, P. H. Chang, W. C. Tseng, *Computers and Structures*, 81 (2003), 273
- B. Petrovski, M. Koçak, *Mis-Matching of Welds*, ESIS 17 (Edited by K. H. Schwalbe, M. Koçak), Mechanical Engineering Publications, London 1994, 511
- F. Jonassen, J. L. Meriam, E. P. Degarmo, *Weld J*, 25 (1946) 9, 492
- E. F. Rybicki, P. A. Mcguire, *Trans ASME J. Eng Mater Technol.*, 104 (1982), 267
- R. L. Koch, E. F. Rybicki, R. D. Strttan, *J. Eng Mater Technol.*, 107 (1985), 148–53
- B. L. Josefson, *Trans ASME J. Press Vessel Technol.*, 104 (1982), 245
- C. Heinze, C. Schwenk, M. Rethmeier, *Journal of Constructional Steel Research*, 19 (2011), 1847
- P. J. Withers, H. K. D. H. Bhadeshia, *Mater. Sci. Technol.*, 17 (2001), 366
- T. Kannengießer, T. Böllinghaus, M. Neuhaus, *Weld World*, 50 (2006), 11
- L. Gannon, Y. Liu, N. Pegg, M. Smith, *Marine Structures*, 23 (2010), 385
- S. W. Wen, P. Hilton, D. C. J. Farrugia, *Journal of Material Processing Technology*, 119 (2001), 203
- P. Michaleries, A. Debicari, *Welding Journal*, 76 (1997), 172
- K. Ogawa, D. Deng, S. Kiyoshima, N. Yanagida, K. Saito, *Computational Materials Science*, 45 (2009), 1031
- L. Tall, *Welding Journal*, 43 (1964), 10
- Y. Ueda, T. Yamakawa, *Proceedings of international conference on mechanical behaviour of materials*, 1971, 10
- R. Karlsson, B. Josefson, *ASME Journal of Pressure Vessel Technology*, 112 (1990), 84